Spatiotemporal nonlinear dynamics of a magnetoelastic ribbon

T. L. Carroll, M. D. Todd, F. J. Rachford, and L. M. Pecora
United States Naval Research Laboratory, Washington, D.C. 20375
(Received 13 November 2000; published 16 April 2001)

Magnetoelastic materials have a strong coupling between strain and magnetization, so applying a magnetic field to a magnetoelastic material can change its shape. This coupling leads to interesting dynamics. We have studied the dynamics of a wide ribbon of Metglass 2605sc which was driven by a magnetic field. The ribbon was suspended as a pendulum in a set of Helmholtz coils, which provided both dc and ac magnetic fields. Laser light was reflected off the ribbon to measure its angular displacement. Two points on the ribbon could be simultaneously illuminated, and one of the laser beams could be scanned over the ribbon. We observed quasiperiodic bifurcations in the motion of the ribbon, and characterized the spatial aspect of the motion with some recently developed statistics.

DOI: 10.1103/PhysRevE.63.056205 PACS number(s): 05.45.Tp

I. INTRODUCTION

The use of a magnetoelastic ribbon to study nonlinear dynamics is quite well known [1,2]. Magnetoelastic materials are easy to work with, and, because they are magnetic, one may drive them without directly touching the material. Most previous experiments with magnetic ribbons used narrow ribbons which could be approximated as one dimensional; in this work, we use a wider ribbon so that we may look for spatial effects. We do see many nonlinear effects, such as a foldover in a mechanical resonance peak, and interesting quasiperiodic bifurcations. We compare the dynamics of a magnetoelastic ribbon to the dynamics of a nonmagnetoelastic ribbon to see what effect the magnetoelasticity has on the ribbon behavior.

The dynamical properties of a magnetoelastic ribbon itself are interesting because the ribbon has applications in technology, but magnetoelastic behavior alone is not our primary reason for the experiments below. The study of the spatial behavior of systems that are temporally chaotic has tended to be limited to simple theory, such as coupled map lattices [3,4], or complicated experiments, such as fluid flow. We wanted to set up a simple tabletop experiment in which we could observe spatiotemporal behavior, both to learn about the spatial behavior of relatively simple systems and to provide data for testing nonlinear analysis algorithms. Magnetic systems are useful for such experiments, because they may be driven without actually contacting the material, because they can be highly nonlinear, and because magnetic materials are easily available. For magnetostrictive materials, interesting dynamics can be seen in the audio frequency range, making experiments simple and relatively inexpensive.

II. MATERIALS

Samples of Metglass 2605sc [5] and 2705m were provided by AlliedSignal Inc. Metglass 2605 has a large magnetostriction (30 ppm saturation magnetostriction), while 2705m has a magnetostriction that is much smaller (much less than 1 ppm), but similar physical properties.

The magnetoelastic coupling in a magnetoelastic material couples the mechanical strain in a material to the magnetic field. The total energy of a magnetoelastic material in a magnetic field is a sum $E_{total}=E_H+E_{anis}+E_{me}+E_{elas}+E_{stress}$, where E_H is the energy due to the interaction between the applied magnetic field and the magnetization of the material, E_{anis} is the energy due to the magnetic anisotropy of the material (the tendency of the magnetization to have a preferred direction), E_{me} is the magnetoelastic coupling energy, E_{elas} is the energy due to the intrinsic stiffness of the material, and E_{stress} is the energy due to an externally applied stress. For a two-dimensional material with a magnetic field H applied along the y axis, an anistropy axis in the x direction, and an externally applied stress σ in the y direction, the total energy may be written

$$E_{Total}=-HM_s\alpha_y-K\alpha_x^2-b(\varepsilon_{xx}\alpha_x^2+\varepsilon_{yy}\alpha_y^2+\varepsilon_{xy}\alpha_x\alpha_y)+\frac{1}{2}C_{11}\varepsilon_{xx}^2+\frac{1}{2}C_{11}\varepsilon_{yy}^2+C_{12}\varepsilon_{xx}\varepsilon_{yy}+\frac{1}{2}\left(\frac{C_{11}-C_{12}}{2}\right)\varepsilon_{xy}^2-\sigma\varepsilon_{yy}, \quad (1)$$

where M_s is the saturation magnetization of the material, K is the anisotropy constant, the C's are elastic constants for the material, the ϵ's are the stresses, b is the magnetoelastic coupling constant, and the α's are the cosines of the angles from the x and y axes [6].

III. EXPERIMENT

The magnetoelastic ribbons were 1 mil thick, and they were made into pieces 25 mm wide by 60 mm long. The ribbons were clamped at the top (across the narrow direction) and suspended as a pendulum, with a 1.6-g mass attached to the bottom (Fig. 1). The ribbons were suspended in a pair of Helmholtz coils which provided a dc bias field of 6 Oe and an ac field of several Oe at frequencies of 3 Hz to several thousand Hz. Both magnetic fields were in the plane of the ribbon, parallel to the narrow direction. A pickup coil within the Helmholtz coils detected the ac magnetic field. The ribbons were not annealed but were used as cast.

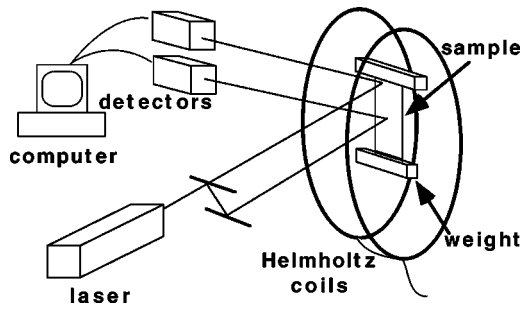

FIG. 1. Diagram of the experiment.

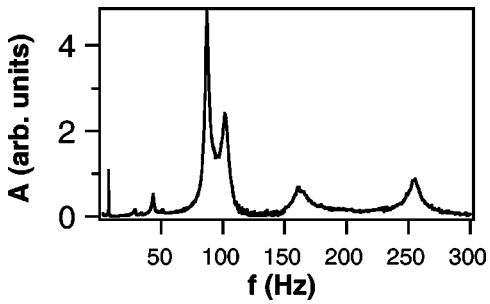

FIG. 2. Amplitude response of a ribbon of nonmagnetostrictive ribbon of Metglass 2705m as a function of driving frequency.

The dc bias field was chosen to maximize the response of the ribbon to the ac driving field. The dc field is small, so the ribbon should still contain magnetic domains. There are two ways in which an ac magnetic field could drive the ribbon: (1) a direct interaction with components of the magnetization not parallel to the ac field will produce a force $\mathbf{F}=\gamma\mathbf{M}\times\mathbf{H}$, and (2) the variation of the direction of the magnetization will affect the shape of the ribbon through the magnetoelastic coupling. It is difficult to determine which of these terms is more important, but the experiments below suggest that both terms have an effect.

Angular deflections of the ribbon were detected by shining a HeNe laser on the ribbon, and detecting the reflected beam. The laser beam was split into two parts so that two points on the ribbon's surface could be illuminated simultaneously. The surface of the ribbon was neither smooth or flat, so the reflected laser beams were diffuse. The light from the reflected beams was directed by mirrors and focused onto two small-area diode detectors. The detectors each contained a second element that monitored the laser output directly in order to cancel any low frequency noise caused by laser fluctuations. The motion of the laser spots across the detectors produced a signal that was proportional to the angular deflection of the ribbon. Because of the varying surface texture of the ribbon, the amplitudes of the detected signals from different points could not be directly compared, although for most of the measurements that we were interested in, relative amplitudes were not important.

IV. MODE SPECTRA

The two-dimensional ribbon can bend out of plane, twist, or stretch. The bending modes have the lowest frequencies, so they are the easiest modes to study. Our ac driving source limited the highest driving frequency to below approximately 10 kHz, which is below the frequency of the axial (stretching) modes. The low order bending modes are within easy reach of our experimental frequency range, so we concentrated on those modes.

Structural modes were computed using a Rayleigh-Ritz technique [7], whereby the bending deflection $w(x,y,z,t)$ of the ribbon is expanded in a series as

$$w(x,y;t)=\sum_{m=0}^{M}\sum_{n=0}^{N} a_{mn}\Psi_m(x)\Phi_n(y), \qquad (2)$$

where $\Psi_m(x)$ and $\Phi_n(y)$ are the classical Euler-Bernoulli clamped-free and free-free beam functions, the latter of which also includes the two rigid body modes, representing the approximate structural boundary conditions of no shear and no moment (free end) and no displacement or rotation (clamped end). Using the expressions for the maximum kinetic (T) and strain energy (U) present in the freely oscillating ribbon,

$$T=\frac{1}{2}\int\int\int \rho w_t^2\, dV,$$

$$U=\frac{D}{2}\int\int (w_{xx}^2+w_{yy}^2)^2-2(1-\nu)(w_{xx}w_{yy}-w_{xy}^2)dA, \qquad (3)$$

where T is computed over the ribbon volume, U is computed over the ribbon planar area, ρ is the mass density of the ribbon, and D is the flexural rigidity of the ribbon. Substitution of Eq. (2) using $M=N=7$ into the Lagrangian $d(T-U)/dt$, with T and U given by Eq. (3), results in a 49×49 truncated eigensystem, whose solution are the modal frequencies (eigenmodes) and modal vector particpation factors (eigenvectors) for the system.

V. EXPERIMENTAL RESULTS

A. Spectrum of modes

We detected bending modes in the experiment by varying the driving frequency between 3 and 300 Hz, and recording the amplitude of the detector output when the laser beam illuminated a fixed spot at the center of the ribbon. Figure 2 shows the amplitude of the detector output for the nonmagnetostrictive 2705m ribbon. The largest mode peak, at 80 Hz, is caused by the natural pendulum motion of the ribbon. The other peaks are due to low order bending modes. The spectrum of the magnetostrictive 2605sc ribbon follows a similar pattern, except that all modes appear to be at slightly lower frequencies. We choose two modes, at frequencies of 129 and 259 Hz, for further study, since their behavior is typical of that seen for the other modes. The 129-Hz mode is not easily visible on the scale of Fig. 2 because the laser spot was near a node for this mode when the frequency scan was made.

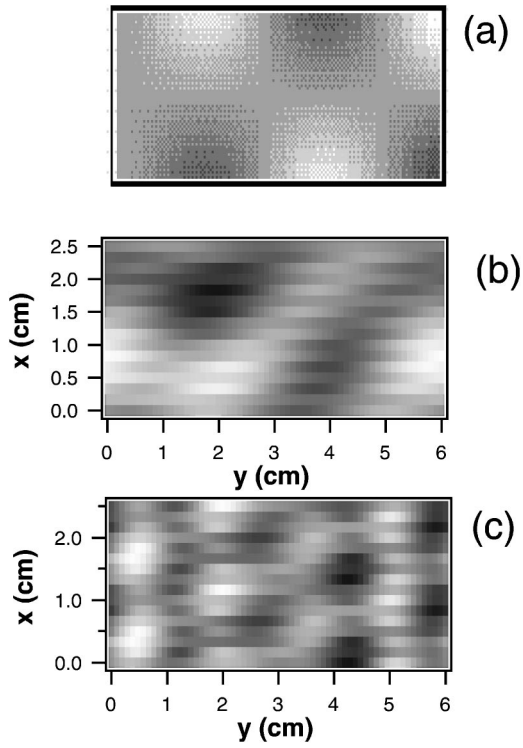

FIG. 3. (a) Calculated mode amplitude of a bending mode at 132 Hz. (b) Experimentally measured phase response (filtered) of a mode at 129 Hz in a nonmagnetostrictive 2705m ribbon. (c) Experimentally measured phase response (filtered) of a mode at 114 Hz in a magnetostrictive 2605sc ribbon.

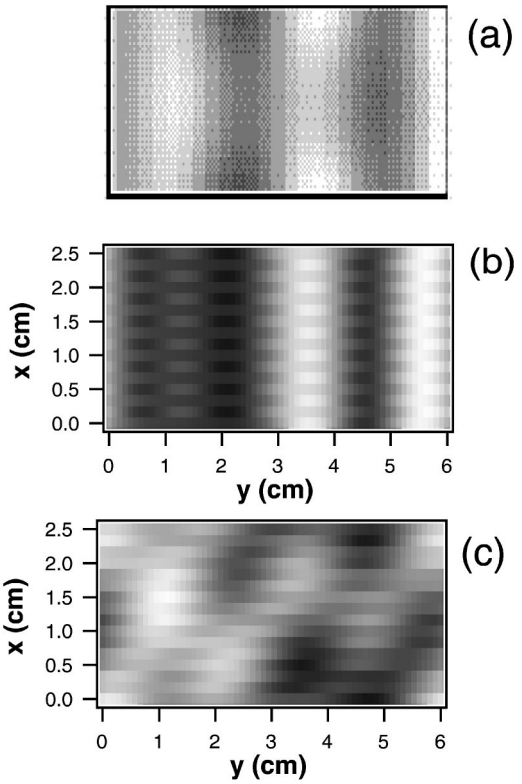

FIG. 4. (a) Calculated mode amplitude of a bending mode at 256 Hz. (b) Experimentally measured phase response (filtered) of a mode at 256 Hz in a nonmagnetostrictive 2705m ribbon. (c) Experimentally measured phase response (filtered) of a mode at 244 Hz in a magnetostrictive 2605sc ribbon.

B. Mode shapes

For each of these modes, we scanned one of the laser spots in a grid pattern over the surface of the ribbon and the phase of the periodic signal at each point was measured relative to the phase of the ac magnetic field. We used a phase measurement, since the amplitude measurements were not comparable from point to point because of the uneven surface of the ribbon. The phase measurements were still somewhat noisy from point to point, so we performed a two-dimensional Fourier transform on the phase data, discarded all but the four Fourier modes with the largest amplitudes, and inverse transformed. Figure 3(a) shows the calculated mode amplitude for the bending mode at 132 Hz, where white is the highest value and black is the lowest. Figure 3(b) is the (filtered) phase plot from the 2705m ribbon for the mode at 129 Hz. We are comparing phase to amplitude, so the plots will look different, but the overall symmetry is approximately the same.

As Fig. 3(c) shows, the corresponding mode for the magnetostrictive 2605sc ribbon looks very different. This phase plot was made for the closest mode, at 114 Hz. The 114-Hz mode in the magnetostrictive ribbon is far more complex than nearby modes in the nonmagnetostrictive ribbon, and in fact appears to look like a higher order mode. This pattern was also seen for other modes in the magnetostrictive ribbon—they were far more complex than modes at similar frequencies in the nonmagnetostrictive ribbon. A second phase plot for this mode was made with a larger dc bias field of 35 Oe. The phase plot for the magnetostrictive ribbon when the bias field was 35 Oe looked essentially the same as the phase plot for the nonmagnetostrictive ribbon when the bias field was 6 Oe, suggesting that the complexity of mode plot for the magnetostrictive ribbon at 6 Oe is caused by magnetic domains. In magnetic materials, the local preferred direction for the magnetic field may be random at low applied fields, so that the magnetization vector for the material points in different directions in different regions (domains) of the material, leading to different mechanical properties for different regions of a magnetostrictive material. Applying a large enough magnetic field will cause the magnetization in different parts of the sample to align, so that the mechanical properties are constant. The 6-Oe field does not appear to be large enough to eliminate the magnetic domains, but the 35-Oe field seems to eliminate most of the domain structure, so that the bending mode looks similar to the calculated mode. Calculating the field necessary to eliminate domains is complicated, and depends on the shape of the material as well as its properties.

Figure 4 shows another set of modes. Figure 4(a) is the calculated mode amplitude for a bending mode with a frequency of 256 Hz. Figure 4(b) is the (filtered) phase plot for the mode at 259 Hz in the nonmagnetostrictive ribbon. Once again, the two plots appear to have the same symmetry. Figure 4(c) is a phase plot for the closest mode in the magnetostrictive ribbon, at 244 Hz. Although this mode does not

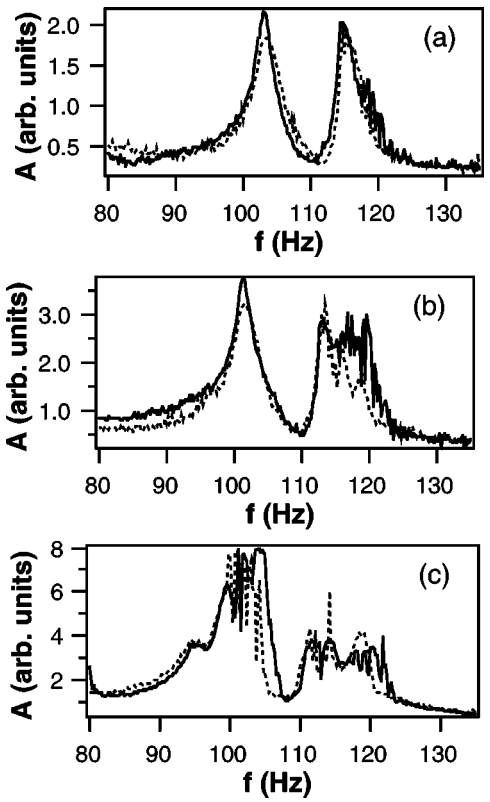

FIG. 5. Amplitude spectrum for the magnetostrictive 2605sc ribbon between 80 and 130 Hz for three different values of the driving magnetic field. The solid line corresponds to sweeping the driving field from low to high frequency, while the dotted line corresponds to sweeping from high to low frequency. (a) The driving field is 0.2 Oe. (b) The driving field is 0.4 Oe. (c) The driving field is 0.8 Oe.

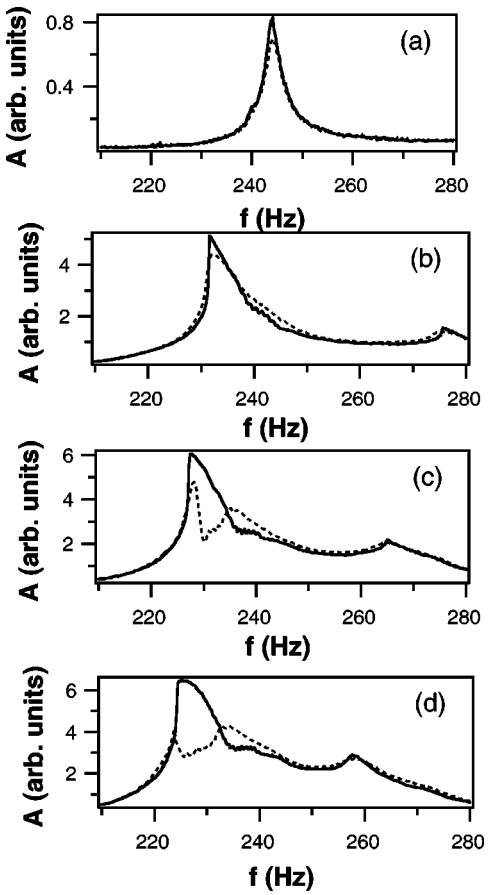

FIG. 6. Amplitude spectrum for the magnetostrictive 2605sc ribbon between 210 and 280 Hz for four different values of the driving magnetic field. The solid line corresponds to sweeping the driving field from low to high frequency, while the dotted line corresponds to sweeping from high to low frequency. (a) The driving field is 0.07 Oe. (b) The driving field is 0.7 Oe. (c) The driving field is 1.05 Oe. (d) The driving field is 1.4 Oe.

appear to have an unusually high order for its frequency, it does not possess the same symmetry as the nearby mode in the nonmagnetostrictive ribbon. Once again, using a larger bias field causes the mode structure in the magnetostrictive ribbon to match the mode structure in nonmagnetostrictive ribbon.

C. Peak shapes: Hysteresis and foldover

The shape of the peaks in the mode spectra also reflects the different nonlinear interactions present in the magnetostrictive ribbon. As we increase the ac driving field to fields as high as 12 Oe peak to peak, the shape of the peaks in the mode spectrum of the nonmagnetostrictive 2705m ribbon does not change, but the shape of the peaks in the mode spectrum of the magnetostrictive 2605sc ribbon does change, reflecting the extra nonlinear interactions caused by the greater magnetostriction of the 2605sc ribbon.

Figure 5 shows the peaks at 104 and 114 Hz in the mode spectrum of the 2605sc ribbon. In Fig. 5(a), the peak to peak ac driving field is 0.2 Oe, in Fig. 5(b) the driving field is 0.4 Oe, and in Fig. 5(c) the driving field is 0.8 Oe. The solid line in Fig. 5 corresponds to sweeping the ac driving frequency from low to high frequency, while the dotted line corresponds to sweeping from high to low frequency. As the ac driving field is increased, the shape of the peaks at 104 and 114 Hz changes a great deal.

Figure 6 shows the peak at 244 Hz as the ac driving field is increased. Once again the solid line means that the ac frequency was scanned from low to high, and the dotted line means that the ac frequency was scanned from high to low. In Fig. 6(a), the driving field was 0.07 Oe peak to peak. In Fig. 6(b), the field was 0.7 Oe, in Fig. 6(c) it was 1.05 Oe, and in 6(d) it was 1.4 Oe. In Figs. 6(b), 6(c), and 6(d), one can see evidence of foldover, a frequency sweep dependent change in shape of a resonance peak that occurs when a resonance frequency is different for high levels of excitation than for low levels. Figure 6 also shows that there is a great deal of hysteresis in the resonance peak for this mode.

D. Bifurcations

Nonlinear effects that may occur in a dynamical system include bifurcations. The wave forms seen when the nonmagnetostrictive 2705m ribbon is driven do include higher harmonics, so some nonlinearity is present, but there are no bifurcations. Bifurcations are seen when the magnetostrictive 2605sc ribbon is driven.

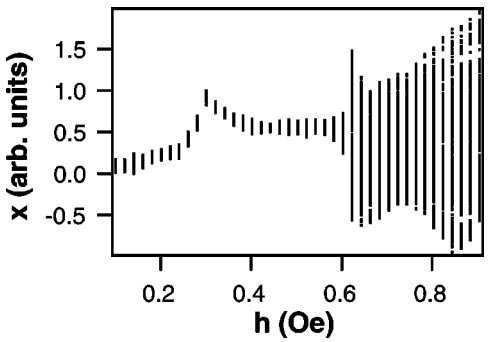

FIG. 7. Bifurcation diagram for the magnetostrictive 2605sc ribbon driven at a frequency of 114 Hz. The peak-to-peak magnetic driving field is h, while x is the value of the detector output when the driving signal crosses zero in the positive direction.

Figure 7 is a bifurcation diagram for the 2605sc ribbon when it is driven at 114 Hz. One of the laser beams is reflected from the center of the ribbon, and the signal from the corresponding detector is digitized every time that the periodic driving signal crosses zero (in the positive direction). The resulting set of points is plotted on the vertical axis at a horizontal value corresponding to the peak to peak driving field.

Figure 7 shows that up to a driving field of about 0.6 Oe, the ribbon motion is periodic. The width of the bifurcation plot below this value is caused by experimental noise. At a driving field of about 0.6 Oe, a bifurcation occurs. Figure 8 shows Poincaré sections taken by strobing the detector output every time that the driving signal crosses zero, going in the positive direction to produce a time series $x(n)$, and then plotting $x(n+1)$ vs $x(n)$. Figure 8(a) is for a driving field of 0.5 Oe, and shows a single point (broadened by experimental noise), implying a periodic response. Figure 8(b) is the Poincaré section at a driving field of 0.7 Oe. Figure 8(b) looks like the cross section of a complicated torus, implying that the motion of the ribbon at 0.7 Oe is quasiperiodic. The nature of the motion is confirmed by the power spectra of Fig. 9. Figure 9 shows power spectra of the strobed time series, so the highest possible frequency is half the strobing frequency, or 57 Hz. Figure 9(a) is the strobed power spectrum at 0.7 Oe, showing that an additional frequency of about 2.2 Hz has appeared in the motion of the ribbon. Power spectra of the continuous signal from the detector confirm that the only added frequency is at 2.2 Hz.

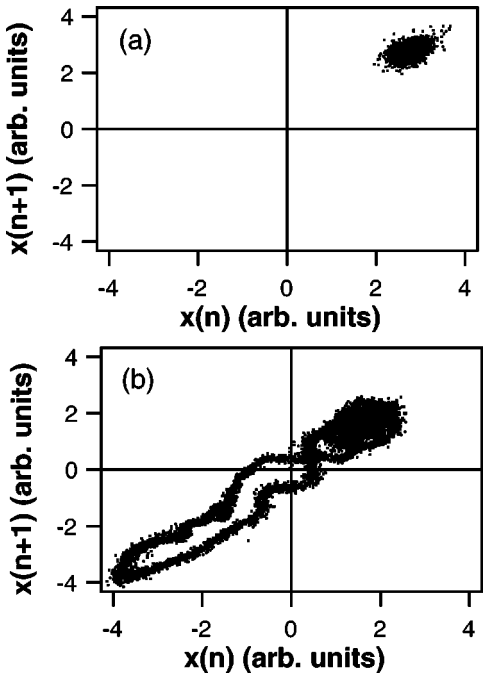

FIG. 8. Poincaré sections for the 2605sc ribbon generated at a driving frequency of 114 Hz. (a) A driving field of 0.5 Oe. (b) A driving field of 0.7 Oe.

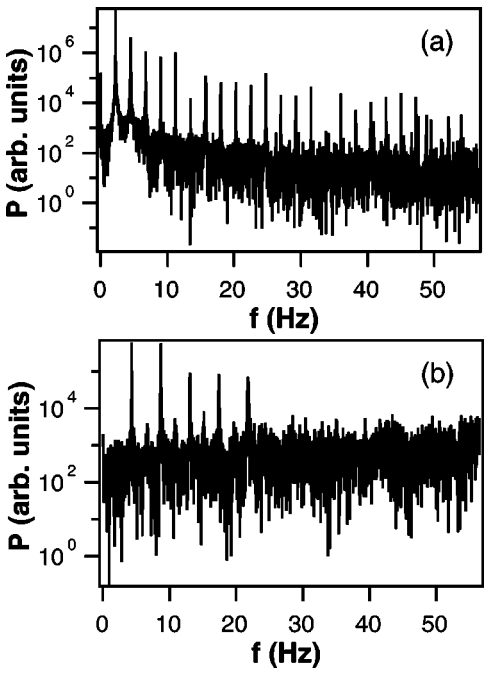

FIG. 9. Power spectra of the strobed detector signal for the 2605sc ribbon driven at 114 Hz. (a) Spectrum at a driving field of 0.8 Oe. (b) Spectrum at a driving field of 2.6 Oe.

Figure 9(b) shows the strobed power spectrum at a driving field of 2.6 Oe. The motion is still quasiperiodic, but now the added frequency is 5 Hz. There is a bending mode in this ribbon at 5 Hz, so the presence of the 5-Hz signal in the motion of the ribbon driven at 114 Hz may represent an interaction between two bending modes.

The same type of bifurcation is seen for the mode at 244 Hz. Figure 10 is a bifurcation diagram for the 244-Hz mode in the magnetoelastic ribbon. The response of the ribbon is periodic up to an ac driving field of about 3 Oe, at which point a bifurcation to quasiperiodic motion occurs. Figure 11(a) shows a Poincaré section from the detected at an ac field just below the bifurcation, while Fig. 11(b) shows a Poincaré section just above the bifurcation. Below the bifurcation the signal is periodic (with some added noise), but above the bifurcation the signal is complex and possibly quasiperiodic. The power spectrum of the strobed signal just above the bifurcation [Fig. 12(a)] confirms that the signal is quasiperiodic, with an added frequency of 2.2 Hz. Figure

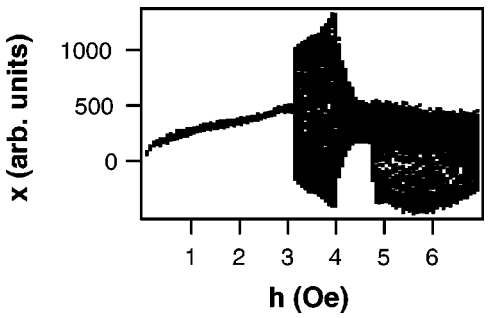

FIG. 10. Bifurcation diagram for the magnetostrictive 2605sc ribbon driven at a frequency of 244 Hz. The peak-to-peak magnetic driving field is *h*, while *x* is the value of the detector output when the driving signal crosses zero in the positive direction.

12(b) shows that the added frequency has increased to 5 Hz by the time that the ac field has increased to 5.4 Oe.

Another bifurcation takes place at approximately 5.7 Oe. The motion of the ribbon begins to oscillate between periodic and quasiperiodic states, with a very slow oscillation frequency. Figure 13 is a long-time plot of the strobed detector signal at this field, showing slow oscillations in the envelope of the signal with a period of about 14 s (about 0.07 Hz). The time scale of the response includes frequencies that vary by a factor of 244/0.7, or approximately 3500.

VI. NONLINEAR STATISTICS

The highly nonlinear nature of magnetoelastic materials makes them difficult to model, especially when they are more than one dimensional. For our system, some modeling may be possible for low driving levels, but for higher driving

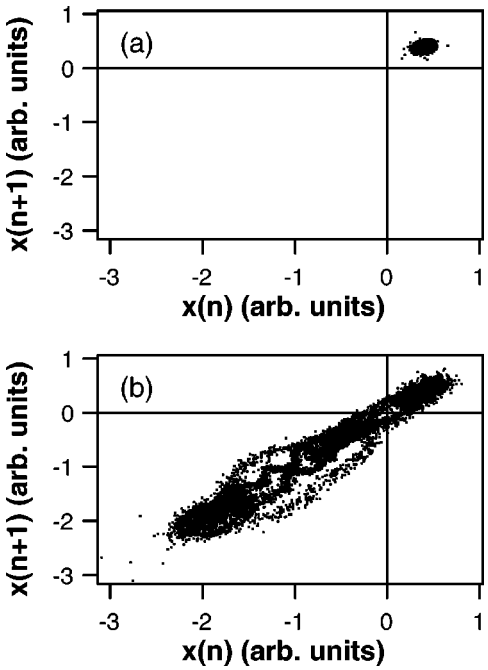

FIG. 11. Poincaré sections for the 2605sc ribbon generated at a driving frequency of 244 Hz. (a) Driving field of 1.3 Oe. (b) Driving field of 3.5 Oe.

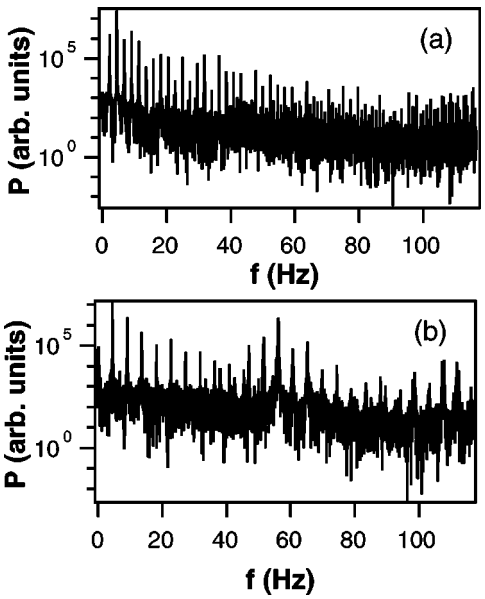

FIG. 12. Power spectra of the strobed detector signal for the 2605sc ribbon driven at 244 Hz. (a) Spectrum at a driving field of 3.5 Oe. (b) Spectrum at a driving field of 5.4 Oe.

levels where some very interesting phenomena occur (such as the very low frequency motion seen in Fig. 13), it is unlikely that accurate modeling will be practical. We may still learn something about the motion of the ribbon at large driving amplitudes by using recently developed statistics to characterize the relation between pairs of nonlinear time series.

A. Description of statistic

In previous work [8], we developed a statistic Θ_{c0} that describes the likelihood that two attractors created by embedding two simultaneous time series are related to each other by a continuous one-to-one function. If $\Theta_{c0}=1$, then the attractors are definitely related by a function; if $\Theta_{c0}=0$, then the attractors are definitely not related.

The method for calculating Θ_{c0} is described in detail in Ref. [8]; we give a brief description here. One time series is embedded to form a source attractor, and one is embedded to form a target attractor. We determine a useful length scale σ on the target attractor by choosing a random center point,

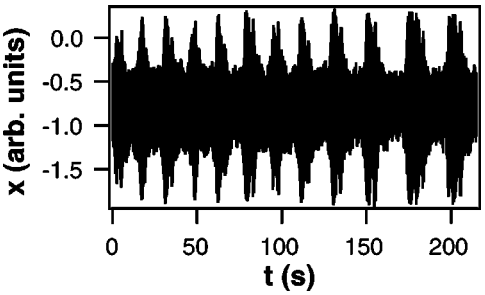

FIG. 13. Time series of the strobed detector signal for the 2605sc ribbon for the mode at 244 Hz, with a driving field of 5.7 Oe.

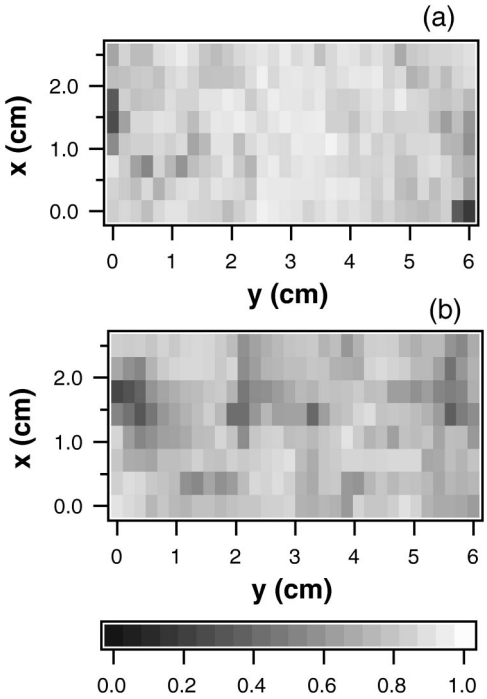

FIG. 14. Plot of statistics relating the strobed signal from the center of the 2605sc ribbon to signals from other points on the ribbon. White represents a value of 1, while black represents a value of 0. The driving field was 1.4 Oe, with a frequency of 114 Hz. (a) Value of the nonlinear statistic Θ_{c0}. (b) Value of the linear cross correlation.

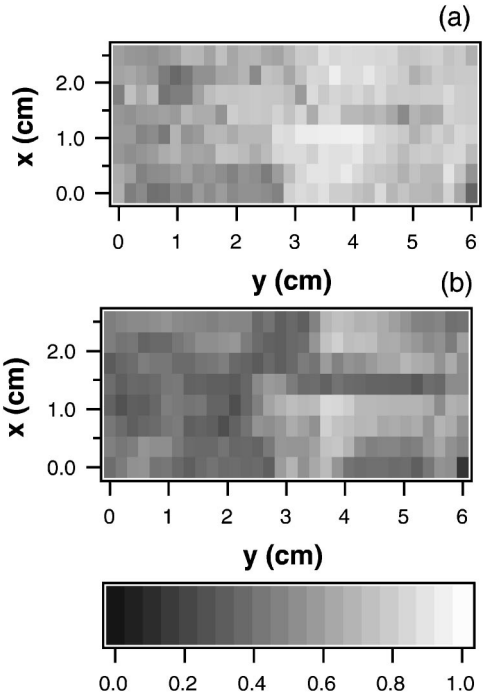

FIG. 15. Plot of statistics relating the strobed signal from the center of the 2605sc ribbon to signals from other points on the ribbon. White represents a value of 1, while black represents a value of 0. The driving field was 6.1 Oe with a frequency of 114 Hz. (a) Value of the nonlinear statistic Θ_{c0}. (b) Value of the linear cross correlation.

finding a set of near neighbors, and calculating the variance for this set of points. If the set of points was simply picked at random, we would expect to find a much larger variance than if the set of points were near neighbors. The variances for all possible sets of points randomly selected on the target attractor fit a Gaussian distribution, so σ is chosen as the average value of this distribution, and σ is varied so that the probability that randomly selecting a group of points with the same variance as the group of neighbors is less than 5%. The same calculation is repeated for many centers, to produce an average σ for the target attractor.

We then pick a random point on the source attractor and find all points within some radius δ of the center point. Because the two time series that generated the attractors were sampled simultaneously, there is a set of points corresponding in time on the target attractor. If the corresponding set of points on the target attractor is also near neighbors, then there is probably a continuous functional relationship between attractors; if the corresponding points are not near neighbors, then there is probably no relationship. The length scale σ that was calculated for the target attractor is used to determine if a group of points are neighbors; if the variance of the group of points is much smaller than σ, then the group of points are probably neighbors, otherwise the group of points are probably not neighbors. The final product of this calculation is an average statistic for the entire attractor, where $\Theta_{c0}=1$ means that there is definitely a functional relation between attractors and $\Theta_{c0}=0$ means that there is definitely not a relationship. Θ_{c0} may also take on values between 1 and 0.

B. Experimental results

One of the time series used to calculate the statistic Θ_{c0} came from a laser beam shining on the center of the ribbon, while the other time series came from a laser beam that was scanned over the surface of the ribbon. The signals from the two detectors were strobed at the driving frequency, so the resulting time series of length 2000 points do not contain terms at the driving frequency. In all of these plots, the top left corner of the ribbon was at the coordinates (0,0), while the reference beam was in the center of the ribbon.

Figures 14 and 15 are for the mode at 114 Hz. The largest embedding dimension calculated from a continuously sampled time series [9] was 3, so to be safe an embedding dimension of 3 was used in order to reconstruct the source and target attractors from the strobed time series (the embedding delay was 1). Figure 14(a) is a plot of Θ_{c0} over the surface of the ribbon when the driving amplitude was 1.4 Oe, where white represents a value of 1.0 and black one of 0.0. Lighter colors predominate, so it appears that in most cases motion on different parts of the ribbon is functionally related to motion in the center of the ribbon. Figure 14(b) shows the linear cross correlation between the same sets of time series, where the linear cross correlation was defined as

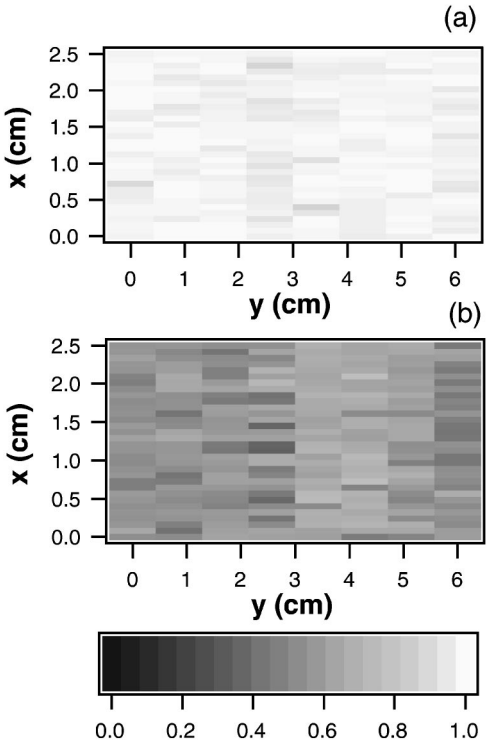

FIG. 16. Plot of statistics relating the strobed signal from the center of the 2605sc ribbon to signals from other points on the ribbon. White represents a value of 1, while black represents a value of 0. The driving field was 3.4 Oe at a frequency of 244 Hz. (a) Value of the nonlinear statistic Θ_{c0}. (b) Value of the linear cross correlation.

$$R = \frac{\sum_{i=1}^{N} (x_i - \overline{x})(y_i - \overline{y})}{\sqrt{\sum_{i=1}^{N} (x_i - \overline{x})^2 (y_i - \overline{y})^2}} \tag{4}$$

where x and y are the two time series.

The cross correlations shown in Fig. 14(b) are not as large as the values of Θ_{c0} in Fig. 14(a), but the cross correlation measures only the linear relation between time series, while Θ_{c0} measures nonlinear relations. Because these statistics were calculated from strobed time series, the periodic driving term did not affect the calculations.

Figure 15 shows these same statistics when the driving amplitude was 6.1 Oe. Figure 15(a) shows the statistic Θ_{c0}, while Fig. 15(b) shows the cross correlation. Both Figs. 1(a) and 1(b) tend to have lower magnitudes than the corresponding statistics in Fig. 14, so it is less certain that the motion at all parts of the ribbon is functionally related to motion at the center. Also in Figs. 15(a) and 15(b) the part of the ribbon for $y<3$ cm is darker than for $y>3$ cm, indicating that the motion in the ribbon is different for the two different regions.

The same statistics for the mode at 244 Hz are shown in Figs. 16 and 17. Figure 16 shows the statistics at a driving field of 3.4 Oe, just above the bifurcation in Fig. 10. Figure 16(a) is the statistic Θ_{c0}, while Fig. 16(b) is the linear cross correlation. Looking only at the linear cross correlation in Fig. 16(b), one would say that there is not much relation between the motion of the ribbon at different points (remember that the statistics were generated from a strobed time series, so the periodic driving term does not influence the cross correlation), but the nonlinear statistic Θ_{c0} in Fig. 16(a) shows that there is a strong functional relation between the motion at different points. The cross correlation only measures linear relations, while the statistic Θ_{c0} is sensitive to nonlinear functions.

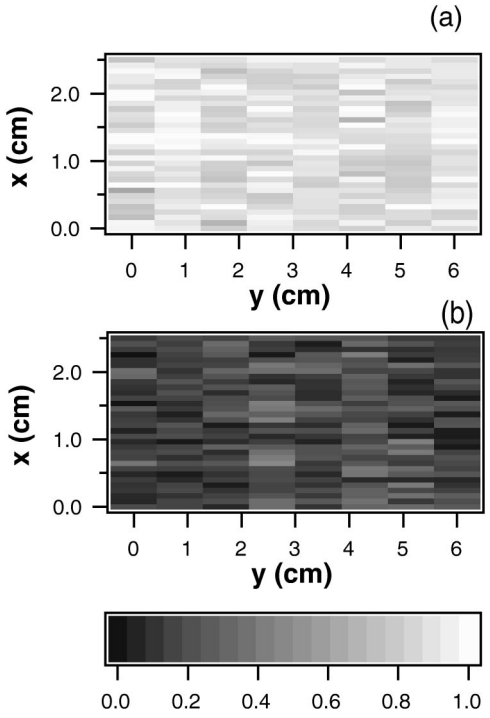

FIG. 17. Plot of statistics relating the strobed signal from the center of the 2605sc ribbon to signals from other points on the ribbon. White represents a value of 1, while black represents a value of 0. The driving field was 6 Oe at a frequency of 244 Hz. (a) Value of the nonlinear statistic Θ_{c0}. (b) Value of the linear cross correlation.

The same pattern appears in Fig. 17, for which the driving field was 6 Oe. The motion seen at this driving field is the same as the motion plotted in Fig. 13; a slow oscillation between periodic and quasiperiodic motions. The cross correlation plot in Fig. 17(b) shows very little cross correlation between the motion at different points on the ribbon, but the statistic Θ_{c0} shows that there is a strong nonlinear relationship between motion at different points.

VII. CONCLUSIONS

A comparison between the magnetostrictive and nonmagnetostrictive ribbons shows that the magnetoelastic interactions defined in Eq. (1) made a large difference in the motion of the driven ribbons. The most distinctive characteristic of the interaction was a bifurcation from periodic to quasiperiodic motion as the driving field increased. The added frequency at the quasiperiodic bifurcation usually corresponded

to the frequency of a lower order mode of the ribbon, suggesting that the driven mode was able to parametrically excite a lower frequency mode. In the expansion used to calculate these bending modes, different modes are not orthogonal to each other, so the presence of an interaction between modes is not surprising, although this interaction was not seen in the nonmagnetostrictive ribbon. At higher driving levels, very low frequency motion that did not correspond to any known modes was present. Nonlinear statistics showed that motions at different points on the ribbon were strongly related to each other, although this relation was highly nonlinear.

ACKNOWLEDGMENT

The authors wish to thank Kristl Hathaway for useful discussions.

[1] W. L. Ditto, S. N. Rauseo, and M. L. Spano, Phys. Rev. Lett. **65**, 3211 (1990).
[2] W. L. Ditto, M. L. Spano, H. T. Savage, S. N. Rauseo, J. Heagy, and E. Ott, Phys. Rev. Lett. **65**, 533 (1990).
[3] R. O. Grigoriev, M. C. Cross, and H. G. Schuster, Phys. Rev. Lett. **79**, 2795 (1997).
[4] C. Beck, Physica D **103**, 528 (1997).
[5] H. T. Savage and M. L. Spano, J. Appl. Phys. **53**, 8092 (1982).
[6] A. Clark and K. Hathaway, in *Handbook of Giant Magnetostrictive Materials* (Academic Press, San Diego, 2000).
[7] S. Timoshenko and J. N. Goodier, *Theory of Elasticity* (McGraw-Hill, New York, 1951).
[8] C. L. Goodridge, L. M. Pecora, F. J. Rachford, and T. L. Carroll (unpublished).
[9] M. B. Kennel, R. Brown, and H. D. I. A. Abarbanel, Phys. Rev. A **45**, 3403 (1992).